



**HAL**  
open science

## Predictions of fruit shelf life and quality after ripening: Are quality traits measured at harvest reliable indicators?

Thibault Nordey, Fabrice Davrieux, Mathieu Léchaudel

### ► To cite this version:

Thibault Nordey, Fabrice Davrieux, Mathieu Léchaudel. Predictions of fruit shelf life and quality after ripening: Are quality traits measured at harvest reliable indicators?. *Postharvest Biology and Technology*, 2019, 153, pp.52 - 60. 10.1016/j.postharvbio.2019.03.011 . hal-03484772

**HAL Id: hal-03484772**

**<https://hal.science/hal-03484772>**

Submitted on 20 Dec 2021

**HAL** is a multi-disciplinary open access archive for the deposit and dissemination of scientific research documents, whether they are published or not. The documents may come from teaching and research institutions in France or abroad, or from public or private research centers.

L'archive ouverte pluridisciplinaire **HAL**, est destinée au dépôt et à la diffusion de documents scientifiques de niveau recherche, publiés ou non, émanant des établissements d'enseignement et de recherche français ou étrangers, des laboratoires publics ou privés.



Distributed under a Creative Commons Attribution - NonCommercial 4.0 International License

1 **Predictions of fruit shelf life and quality after ripening: Are quality traits measured at harvest**  
2 **reliable indicators?**

3

4 Thibault Nordey<sup>1,2</sup>, Fabrice Davrieux<sup>3,5</sup>, Mathieu Léchaudel<sup>4,5</sup>

5

6 <sup>1</sup>TheWorld Vegetable Center, Eastern and Southern Africa, P.O. Box 10, Duluti, Arusha, Tanzania

7 <sup>2</sup>CIRAD, UPR Hortsys, 34398 Montpellier, France

8 <sup>3</sup>CIRAD, UMR QUALISUD, F-97455 Saint Pierre, La Réunion, France

9 <sup>4</sup> CIRAD, UMR QUALISUD, F-97130 Capesterre-Belle-Eau, Guadeloupe, France

10 <sup>5</sup>QualiSud, Univ Montpellier, CIRAD, Montpellier SupAgro, Univ d'Avignon, Univ de La Réunion,  
11 Montpellier, France.

12

13

## 14 **Abstract**

15 Nondestructive methods such as near infrared spectroscopy (NIRS) are increasingly used in sorting  
16 lines to assess quality traits of unripe fruit, i.e. dry matter (DM) and total soluble solid (TSS) contents,  
17 in order to create homogenous batches of fruit. The use of this approach is based on the assumption  
18 that fruit quality traits at harvest are reliable indicators of their post-harvest behavior and their  
19 quality after ripening. The present study tested this assumption by analyzing the relationships  
20 between quality traits at harvest and after ripening. In parallel, models were developed to determine  
21 the capacity of NIRS measurements on unripe fruit at harvest to predict their shelf life and quality  
22 after ripening.

23 The quality traits DM, TSS content, pulp color (PC) and titratable acidity (TA) of 92 mangoes from  
24 different harvests, production years, and orchards were compared at harvest and after ripening.  
25 Previously developed NIRS models were used to nondestructively assess the quality traits of the  
26 mangoes at harvest. New partial least squares (PLS) regressions using different variable selection  
27 procedures and preprocessing techniques were used to predict fruit shelf life and fruit quality after  
28 ripening based on NIRS measurements at harvest.

29 Weak relationships ( $r^2 < 0.41$ ) were found between fruit quality traits measured at harvest and after  
30 ripening, except for DM content ( $r^2 = 0.61$ ). The PC of mango measured at harvest was found to be  
31 the best indicator of fruit shelf life. Errors of PLS regressions to predict the TSS content (RMSEV =  
32 1.1%), titratable acidity (RMSEV = 0.52%), and the Hue angle of the flesh (RMSEV = 1.86 °) were in the  
33 same range as those of linear regressions based on quality traits assessed at harvest except for PC.  
34 This work provides evidence that fruit maturity and quality should be assessed using different  
35 indicators.

36

37 **Keywords:** *Mangifera indica*; Near-infrared spectroscopy; Non-destructive prediction; Eating quality;

38 PLSR

## 39 **Introduction**

40 The heterogeneity of quality and maturity of fruit at harvest is a widespread problem in numerous  
41 species that needs to be addressed all along the supply chain to reduce postharvest losses and to  
42 insure constant quality for consumers. After harvest, fruit are generally sorted and graded to create  
43 homogenous batches based on the assumption that their post-harvest behavior and quality will be  
44 similar after ripening. To improve quality assessments based on visual rating, i.e. absence of defects,  
45 size, color and shape, several nondestructive methods have been developed to assess other fruit  
46 quality descriptors at the time of measurement such as total soluble solid (TSS) content, titratable  
47 acidity (TA), and the dry matter (DM) content. These methods include the electronic nose (Lebrun *et al.*,  
48 2008), near infrared spectroscopy (NIRS) (Jha *et al.*, 2012a; Nordey *et al.*, 2017; Saranwong *et al.*,  
49 2004; Subedi *et al.*, 2007), visual spectroscopy (Jha *et al.*, 2006), and specific gravity (Kapse and  
50 Katrodia, 1996). Sorting fruit using quality traits measured at harvest assumes that the fruit  
51 composition at this stage is a reliable descriptor of its quality after ripening, and of its shelf life, i.e.  
52 the length of the period between harvest and the ripe fruit stage. This assumption relies on the fact  
53 that the quality of ripe fruit is determined at harvest since the accumulation of dry matter and water  
54 in fruit stops once the fruit is picked. Fruit dry matter contains the preliminary metabolites and  
55 precursors of secondary metabolites that undergo considerable changes during fruit ripening and  
56 hence determine the quality of ripe fruit. In a few days, ripening processes increase fruit quality to its  
57 optimum, which then decline until the fruit become inedible due to over ripening. Metabolic  
58 pathways of preliminary and secondary metabolites are controlled by a balance of different  
59 phytohormones, including ethylene, abscisic acid and gibberellins. The metabolism of these  
60 phytohormones and their involvement in ripening processes are used to differentiate climacteric  
61 fruit from non-climacteric fruit. Managing fruit shelf life is essential to insure optimum fruit quality  
62 for consumers, especially in the case of highly perishable climacteric fruit such as mango, banana and  
63 avocado. The shelf life and the quality of fruit after ripening are known to be closely related to their  
64 stage of maturity at harvest since the shelf life of fruit harvested early is longer but their quality is

65 reduced, i.e. they are smaller, have a lower sugar content, paler pulp, than fruit harvested later (Joas  
66 *et al.*, 2012; Nordey *et al.*, 2016).

67 Although the quality of fruit varies considerably with their stage of maturity, this does not mean that  
68 fruit composition is a reliable indicator of fruit maturity since the concentration of primary and  
69 secondary metabolites is known to vary considerably depending on the growing conditions, e.g.  
70 irrigation, the fruit to leaf ratio, and the position of the fruit in the canopy (Léchaudel and Joas,  
71 2007). For this reason, several studies on mango (Lechaudel *et al.*, 2010), papaya (Urbano Bron *et al.*,  
72 2004), and apple (Song *et al.*, 1997) preferred to use the optical properties of chlorophyll in the fruit  
73 peel assessed with a fluorometer as an indicator of fruit maturity rather than fruit quality descriptors.  
74 Although several studies on mango (Saranwong *et al.*, 2004; Subedi *et al.*, 2007), apple (Palmer *et al.*,  
75 2010), and kiwifruit (Jordan *et al.*, 2000; McGlone *et al.*, 2002b) focused on the relationship between  
76 DM content and TSS content at harvest and after ripening, few investigated relationships with other  
77 quality traits such as TA and pulp color (PC), which are also of importance in consumers' perception  
78 of quality.

79 The first objective of the present study was to investigate the validity of the assumption that fruit  
80 quality descriptors measured at harvest are reliable indicators of the shelf life of fruit and of their  
81 quality after ripening. Mango was used as a model since numerous studies have underlined the  
82 capacity of NIRS measurements to non-destructively measure several fruit quality traits in mango:  
83 TSS content, dry matter content, titratable acidity and pulp color (Cortés *et al.*, 2016; Jha *et al.*,  
84 2012b; Marques *et al.*, 2016; Nagle *et al.*, 2010; Nordey *et al.*, 2017; Rungpichayapichet *et al.*, 2016;  
85 Schmilovitch *et al.*, 2000). We took advantage of previously developed NIRS models to analyze the  
86 relationships between the quality traits measured at harvest and after ripening in a set of mango  
87 fruit sampled from different orchards, harvests and production years. Although numerous studies on  
88 mango focused on the use of NIRS to measure fruit quality traits (see above mentioned studies) and  
89 maturity (Cortés *et al.*, 2016; Nagle *et al.*, 2010; Rungpichayapichet *et al.*, 2016; Subedi *et al.*, 2007)  
90 at the time of measurement, only a few investigated the potential of NIRS measurements at harvest

91 to predict the quality of ripe fruit (Subedi et al., 2007) and shelf life. The second aim of this study was  
92 thus to evaluate the accuracy of NIRS measurements for such predictions. The results of this study  
93 should help stakeholders of fruit value chains choose reliable indicators to assess fruit shelf life and  
94 quality after ripening.

95

## 96 **Material and methods**

### 97 Samples

98 A total of 92 mango fruit (*Mangifera indica* cv. 'Cogshall') harvested during the 2010–2011 and 2014–  
99 2015 production seasons in four orchards in the northwest, west and southwest of Reunion Island  
100 (20°52'48''S, 55°31'48''E) were used. Tree size, spacing and ages differed between orchards, as did  
101 fertilization, irrigation and pruning. Fruit were harvested between 90 and 120 days after full bloom to  
102 account for the wide range of variation in the stage of maturity at harvest from the green mature to  
103 the yellow point stage considered as the onset of fruit ripening for Cogshall mangoes (Lechaudel et  
104 al., 2010). A NIR spectrum was collected for each fruit at harvest, after which the fruit was weighed  
105 and left to ripen at 20 °C and 80% relative humidity (RH).

106 The mangoes were destroyed for composition analysis after ripening. To ensure that ripe fruit was  
107 the same physiological age for analysis, respiratory metabolism and climacteric rise were used as  
108 indicators. Previous studies on the Cogshall cultivar (Joas *et al.*, 2009; Joas et al., 2012; Joas *et al.*,  
109 2010) showed that the fruit quality traits TSS content and TA, firmness vary according to the  
110 climacteric stage of the fruit. In line with these studies, mangoes were considered to be ripe with  
111 correct quality and taste three days after they had reached their highest respiration rate. Respiration  
112 rates were measured daily on each fruit by placing the mango in an individual 3 L airtight jar, and CO<sub>2</sub>  
113 concentration was measured at 20 min intervals for 1 hour by gas chromatography using an Agilent  
114 M200 instrument (SRA, Marcy l'Etoile, France).

### 115 Measurements of fruit quality

116 At the ready to eat stage, mango cheeks were cut off longitudinally to measure the PC with a Minolta  
117 Chroma Meter CR300 (Konica Minolta, Osaka, Japan) and described using the Hue angle criterion.  
118 Variations in TA, DM content and TSS content within mangoes (Nordey *et al.*, 2014) were taken into  
119 account through measurements made on a puree obtained by blending the fruit flesh in a Grindomix  
120 blender (Retsch, Haan, Germany). Fresh juice was extracted by filtering the puree through gauze to

121 measure the TSS content using an ATC-1E refractometer (Atago, Tokyo, Japan) and TA. TA, expressed  
122 as mass percentage of citric acid (%), was measured using an automated titrimer (TitroLine easy,  
123 Schott, Mainz, Germany) with a 0.05 mol L<sup>-1</sup> NaOH solution. The DM content of the flesh was  
124 calculated from the dry mass measured after lyophilization compared with fresh mass.

### 125 Chemometrics

126 At harvest, NIR spectra measurements were collected on the surface of the fruit near the apex over  
127 the 600–2300 nm wavelength range using a portable spectrometer equipped with a contact probe  
128 (LABSPEC 2500, Analytical Spectral Devices, Inc., Boulder, CO, USA). In line with our previous studies  
129 NIR measurements were made on the fruit apex since peel color changes in this part of the fruit is  
130 used as an indicator of the fruit maturity for cogshall mangoes (Lechaudel et al., 2010; Nordey et al.,  
131 2017).

132 NIR measurements were used to non-destructively measure the fruit quality traits DM, TA, TSS and  
133 PC at harvest using previously developed partial least square (PLS) models (Nordey et al., 2017). The  
134 accuracy of the models was expected to be satisfactory since they were calibrated on mangoes taken  
135 from similar orchards in the same year of production as the ones used in the present study. Spectral  
136 measurements collected at harvest were also used to predict the shelf life of the fruit and their  
137 quality after ripening by establishing new PLS models.

138 Samples were divided into calibration and validation sets at an 80:20 ratio for each quality trait  
139 evaluated, i.e., DM and TSS content, PC and TA, by random sampling on percentiles of the quality  
140 attribute values. Partial least squares regressions (PLSR) were established using the PLS package  
141 (Mevik and Wehrens, 2007) of the R software (R Development Core Team, 2012) using the  
142 methodology described by (Cornillon, 2010). The number of PLSR factors was determined to reduce  
143 the prediction error by cross validation on 20% of the calibration set using the mean square error of  
144 prediction as an indicator.

145 Several spectral data pre-processing and variable selection methods developed in our previous study  
146 (Nordey et al., 2017) were tested to improve the prediction performance of PLSR. The preprocessing

147 methods tested were first and second derivatives using the Savitzky-Golay smoothing filter with a  
148 second-order polynomial and a 10-nm window size using the prospectr package (Stevens and  
149 Ramirez-Lopez, 2013). Interval partial least square (IPLS) regressions, associated with the stepwise  
150 and the backward methods, were performed to select the combination of wavelength windows that  
151 best predicted performance. Algorithms for IPLS regressions were designed following the  
152 methodology presented by Andersen and Bro (2010). As proposed by Nicolai *et al.* (2007), the root  
153 mean square error (RMSE) was used as an indicator to evaluate the predictive performance of PLSR  
154 using the calibration (RMSEC) and prediction (RMSEP) datasets.

### 155 Statistical analysis

156 Covariance analyses were performed to assess the impacts of growing conditions, i.e. years of  
157 production and orchards, on relationships between quality traits measured at harvest and after  
158 ripening.

159 A principal component analysis (PCA) was performed to analyze variations in raw NIR spectra  
160 collected on fruit at harvest using the FactoMineR package (Lê *et al.*, 2008). Fruit shelf life was  
161 plotted as a supplementary categorical variable and the positions of the shelf life categories were  
162 plotted on the PCA plot with their confidence ellipses at 95%. Simple and multiple linear regressions  
163 were calibrated and tested using the same calibration and prediction data sets as those used for  
164 PLSR. A variable selection procedure was applied to the accuracy of multiple linear regressions  
165 following the methodology suggested by Cornillon (2010) based on the LEAPS package (Lumley and  
166 Miller, 2009) and on the Bayesian information criterion (BIC). The root mean square error (RMSE)  
167 was used as an indicator to evaluate the predictive performance of linear regressions for the  
168 calibration (RMSEC) and prediction (RMSEP) datasets. A relative RMSEP was calculated as the ratio  
169 between the RMSEP and the mean of all measurements.

170

## 171 Results

### 172 Changes in fruit quality attributes between harvest and after ripening

173 Figure 1 shows the relationships between the fruit quality traits TSS content, dry matter content, TA  
174 and PC measured at harvest using NIRS spectra and after ripening using destructive measurements.

175 Results revealed marked variations in quality at harvest since fruit weight varied between 170 g and  
176 665 g (data not shown), TSS content varied between 4.5 and 20%, TA varied between 2.25 and  
177 12.22%, DM content varied between 12.2 and 23.9%, the hue angle of the PC varied between 83.5  
178 and 116.7 °. Fruit were ripe from two to 17 days after harvest and their fresh mass varied between  
179 156 and 637 g (data not shown), DM content varied between 10.8 and 21%, TA varied between 0.35  
180 and 4.35%, TSS content varied between 10.2 and 22%, and the hue angle of the PC varied between  
181 80.15 and 92.7 °. Weak relationships were found ( $r^2 < 0.41$ ) between quality traits at harvest and  
182 after ripening, except for DM content ( $r^2 = 0.61$ ). The TSS content in ripe fruit was correlated ( $r^2 =$   
183 0.67, Figure 1E) with the DM content measured at harvest, in contrast to TA (Fig. 1F) and PC (Figure  
184 1G).

185 The fruit shelf life was related to the PC ( $r^2 = 0.7$ , Figure 1J) and to the TSS content ( $r^2 = 0.62$ , Fig. 1H)  
186 and to a lesser extent to TA ( $r^2 = 0.5$ , Figure 1I) and to the DM content ( $r^2 = 0.45$ , Figure 1K) measured  
187 at harvest. All relationships established between quality traits measured at the harvest and after  
188 ripening were found to vary significantly with growing conditions, i.e. the year of production and/or  
189 the orchard.

190 The accuracy of linear regressions between quality traits at harvest and after ripening is shown in  
191 Table 1. The variable selection procedure made it possible to increase the accuracy of multiple linear  
192 regressions to predict fruit quality traits after ripening. This approach showed that PC and DM  
193 content of the ripe fruit were best predicted using DM content at harvest as the only indicator.  
194 Although the TSS content in ripe fruit was well predicted using DM content at harvest as the only  
195 explanatory variable, our results showed that including TA and PC in the multiple linear regression  
196 slightly increased prediction accuracy. TA of fruit after ripening was found to be best predicted using

197 PC and TA measured at harvest. In line with previous results, PC at the harvest was shown to be the  
198 best indicator of fruit shelf life.

199

### 200 Use of NIRS measurements at harvest to predict the quality of ripe fruit and shelf life

201 NIRS spectra measured on fruit from 600 nm to 2,300 nm at harvest (Figure 2A) were used to predict  
202 their shelf life at 20 °C and 80% RH, as well as their quality traits after ripening.

203 Reflectance spectra acquired at harvest varied with the shelf life of the fruit (Figure 2A) and a  
204 principal component analysis on raw NIR spectra was performed to highlight these variations (Figure  
205 2B). Principal component analysis revealed more variation in the NIR spectra acquired on fruit with a  
206 longer shelf life.

207 PLSR were developed to predict the quality of fruit after ripening and their shelf life at harvest using  
208 NIR measurements. The results of the preliminary analyses displayed in Figure 3A to 3E underline the  
209 difference in the capacity of NIR windows to predict fruit quality traits and shelf life. These figures  
210 also show that quality traits in ripe fruit are linked to different regions in the NIR spectra. Different  
211 data preprocessing methods (first and second derivative) as well as variable selection procedures  
212 (IPLS backward and stepwise) with different sized windows in the NIR spectra (10, 25, 50 and 100)  
213 were used to increase the prediction accuracy of PLSR (Table 2). The models with the least prediction  
214 errors were selected for the calibration and validation datasets. Models with similar accuracy but  
215 fewer factors were selected to increase the robustness of the results. In line with Figure 3A to 3E,  
216 different regions in the NIR spectra were selected in the models to predict quality traits (Figure 3F to  
217 3J). Predictions of the TSS content in ripe fruit were found to rely on reflectance measurements at  
218 harvest from 1,000 nm to 1,200 nm, as well as on reflectance measurements around 1,800 nm.

219 Similar results were found for DM content since reflectance measurements around 1,000 nm were  
220 selected by the variable selection procedure to predict this trait. Predictions of PC and TA in ripe fruit  
221 were both related to measurements in the NIR region from 1,600 to 1,800 nm. Reflectance

222 measurements in the visible region (around 800 nm) were found to be of importance only for the  
223 prediction of fruit shelf life.

224 Prediction accuracies of the selected PLSR are shown in Figure 4. A RMSEP of 1.1%, 0.52%, 1.86 °,  
225 1.26% and 1.78 days were found for the TSS content, TA, the hue angle of the PC, DM content and  
226 the shelf life, respectively. Marked discrepancies were found between the accuracy of models since  
227 relative RMSEP of 6.9%, 46%, 2.1%, 8%, 18.3%, and 18.3% were obtained for the TSS content, TA, the  
228 hue angle of the PC, DM content, and the shelf life, respectively.

229 Errors of the same order of magnitude were obtained when predicting quality traits and shelf life  
230 using PLSR and linear regressions based on the quality traits assessed at harvest, except for the PC,  
231 i.e. RMSEV = 1.86 ° versus 3.17 °.

232

233

234

## 235 Discussion

### 236 Are fruit quality traits at harvest reliable indicators of fruit shelf life and quality after ripening?

237 Our results show that the color of the pulp is a good indicator of fruit shelf life (Fig. 1J, Table 1).  
238 This result is in line with previous measurements made on mango by Subedi *et al.* (2007), who  
239 reported that fruit maturity was better correlated with PC ( $r^2 = 0.79$ ) than with DM content ( $r^2 =$   
240  $0.66$ ). Previous studies showed that the color of mango flesh is closely linked with its carotenoid  
241 contents (Vasquez-Caicedo *et al.*, 2005), mostly represented by all-trans-carotene, all-trans-  
242 violaxanthin, and 9-cis-violaxanthin (Litz, 2009; Rosalie *et al.*, 2015). The biosynthetic carotenoid  
243 pathway is known to be triggered during fruit ripening leading to marked changes in the color of the  
244 mango flesh. The better capacity of PC to predict the fruit shelf life than the other traits studied  
245 could be explained by the lower sensitivity of the carotenoid metabolism to fruit growing conditions  
246 than the sensitivity of sugars and acids (Joas *et al.*, 2012; Rosalie *et al.*, 2015) and by the impact of  
247 phytohormones in the carotenoid metabolism that drive fruit ripening (McAtee *et al.*, 2013).

248 Not surprisingly, our results showed that fruit DM contents at harvest and after ripening were  
249 closely correlated. Although the composition of fruit DM undergoes major changes during ripening,  
250 its content varies only slightly due to water losses and fruit respiration (Nordey *et al.*, 2016).  
251 During ripening, the starch that accumulates in mangoes throughout their development on the tree  
252 is converted into soluble sugars, i.e., saccharose, glucose and fructose, thereby increasing the fruit  
253 TSS content (Léchaudel *et al.*, 2005). In line with the results of previous studies (Saranwong *et al.*,  
254 2004; Subedi *et al.*, 2007), our results indicated that TSS content at the harvest is not a reliable  
255 indicator of the TSS content in fruit after ripening, which is better predicted by DM content at  
256 harvest. Several modeling approaches have been developed on mango (Léchaudel *et al.*, 2007),  
257 peach (Lescourret *et al.*, 2011), and tomato (Liu *et al.*, 2007) to predict changes in fruit DM during  
258 fruit growth and ripening. These models predict the DM composition of fruit by simulating changes in  
259 the fruit maturity stage and its dry mass balance. Empirical relationships used in the modeling  
260 approaches developed on mango can roughly predict mango glucose, fructose and sucrose contents,

261 and malic, citric, pyruvic and oxalic acid contents, since correlation coefficients ( $r^2$ ) obtained between  
262 predictions and observations ranged between 0.43 and 0.66 (Léchaudel *et al.*, 2007). One of the main  
263 problems involved in predicting changes in the composition of fruit DM is simulating the impacts of  
264 ripening. Further work combining modelling approaches to simulate the metabolism of  
265 phytohormones involved in fruit ripening (Génard and Gouble, 2005) and their impacts on metabolic  
266 pathways of primary and secondary metabolites is thus needed to better predict changes in the DM  
267 composition of the fruit during ripening.

268 In contrast to TSS content, fruit TA after ripening was poorly correlated with predicted fruit DM  
269 content at harvest (Figure 3F). Numerous organic acids are responsible for variations in TA in mango,  
270 but citric and malic acids are known to have the most influence (Léchaudel *et al.*, 2005; Medlicott  
271 and Thompson, 1985). Some modelling approaches have also been developed to simulate TA and the  
272 pH in fruit flesh during fruit growth and ripening (Etienne *et al.*, 2013; Lobit *et al.*, 2003). These  
273 approaches are hampered by the number of organic acids in fruit and by the lack of knowledge on  
274 the mechanisms involved in their metabolism and storage. These models succeeded in underlining  
275 the close relationship between organic acid metabolism and fruit respiration. This relationship was  
276 used by our team to hypothesize that the observed variations in TA among mangoes after ripening  
277 can be partly explained by differences in the climacteric respiratory crisis observed between fruit,  
278 depending on their stage of maturity at harvest (Nordey *et al.*, 2016). Interestingly, the multiple  
279 linear relationships we established in the present study (Table 1 ) reinforce this hypothesis, since, as  
280 mentioned above, TA in the fruit after ripening was better predicted using both TA and PC at  
281 harvest, and the latter was the best indicator of fruit maturity (Table 1, Figure 1J).

282 Like TA, PC after ripening was poorly correlated with DM content and PC at harvest. This is in  
283 agreement with the results obtained by Joas *et al.* (2012), who already underlined the lack of  
284 proportionality between the carotenoid content in fruit at harvest and in ripe fruit (Figure 1C). In  
285 contrast to DM and TSS contents, these authors reported that the carotenoid content in mango flesh  
286 at harvest did not vary either with the fruit carbon supply (Joas *et al.*, 2012) or with the fruit water

287 supply (Rosalie et al., 2015) but did vary with the stage of maturity at harvest (Joas et al., 2012). The  
288 impact of carbohydrate availability in fruit on the metabolism of carotenoids was discussed by  
289 Poiroux-Gonord *et al.* (2012), who suggested that carotenoid biosynthesis was not promoted by  
290 higher concentrations of carbohydrate precursors. Our results confirm their hypothesis, since PC  
291 after ripening was not correlated with TSS or DM content at harvest.

292 Finally, the results of the present work confirm that fruit DM content at harvest is a reliable  
293 indicator of TSS content in ripe fruit, which is known to be closely correlated with their sugar content.  
294 Nondestructive measurements such as specific gravity and NIRS have already been successfully used  
295 to accurately predict the DM content of several fruit species including mango (Nordey et al., 2017;  
296 Saranwong et al., 2004) and kiwi (Jordan et al., 2000; McGlone et al., 2002b). In the present study, all  
297 relationships between fruit quality traits at harvest and after ripening were found to vary with fruit  
298 growing conditions, i.e. with the orchard and/or year of production. To avoid the need to develop  
299 specific relationships for each growing condition, the robustness of these linear regressions could be  
300 improved by including samples of several seasons and growing regions within the  
301 calibration.

302 Our results also showed that DM content at harvest was not a reliable indicator of TA or PC after  
303 ripening. The PC at harvest was found to be the best indicator of fruit shelf life. TA in ripe fruit was  
304 found to be linked to PC and TA at harvest, suggesting that it varied with the stage of maturity at  
305 harvest. Our results underline the fact that although the stage of maturity of fruit and their quality  
306 are closely related, they should not be assessed using the same indicators.

307

### 308 Use of NIRS to predict fruit quality after ripening and shelf life at harvest

309 Unlike other nondestructive measurements such as weight or density, NIRS spectra are collected in  
310 specific locations in the fruit. Like in previous studies (Lechaudel et al., 2010; Nordey et al., 2017) NIR  
311 measurements were made on the fruit apex, whereas in other studies, measurements were made on  
312 the mango shoulders (Saranwong et al., 2004), or in the center of the fruit cheek (Rungpichayapichet

313 et al., 2016), or at several different locations (Jha *et al.*, 2014; Marques et al., 2016). Since marked  
314 variations in both mango quality and maturity were measured previously (Nordey et al., 2014), we  
315 would have expected predictions of quality and maturity to vary according to the position the  
316 measurements were made on the fruit. In contrast to previous studies (Nordey et al., 2014;  
317 Saranwong et al., 2004), NIR measurements collected in the present study were used to predict the  
318 quality and maturity of the fruit as a whole and not of the fleshy part of the measuring area. It is so  
319 assumed through the approach used in the present study that quality and maturity in the apex part  
320 of the fruit are reliable indicators of the quality and maturity of the whole mango. It is worth noting  
321 that automation of the proposed method would be hampered by the need of make NIR  
322 measurements at a specific position on the fruit. However, this challenge could be overcome by  
323 developing new models based on several NIR spectra randomly collected on the fruit surface.  
324 The accuracy of predictions of fruit quality after ripening made at harvest using NIRS spectra (Table  
325 2) was found to be of the same order of magnitude as linear regressions based on the prediction of  
326 quality attributes at harvest, except for the color of the pulp, i.e. RMSEV = 1.86 ° versus 3.17 °.  
327 In contrast to other quality attributes, the accuracy of PLSR to predict TSS content in fruit after  
328 ripening was lower than the accuracy of PLSR previously developed to predict the fruit quality at the  
329 time of measurement: 1.1% versus 0.6%. This can be explained by the smaller difference in quality  
330 attributes between ripe fruit than between unripe fruit harvested at different stages (from green  
331 mature to fully ripe).

332 Like in other fruit, mango spectra were dominated by a water spectrum with overtone bands of OH  
333 bonds at 970, 1450 nm and a combination band at 1940 nm (Figure 2)(Nicolai et al., 2007). The near  
334 infrared spectrum of mango is also composed of overtones and combination bands of organic  
335 compounds. In line with previous studies, NIR measurements made at harvest at around 1000 nm  
336 played an important role in predicting dry matter content and TSS content in ripe mangoes. This  
337 region of the NIR spectra was linked to overtone starch at 990 nm. This result supports the results

338 previously obtained by Saranwong *et al.* (2004) suggesting that the starch content of mango at  
339 harvest is a good indicator of TSS content in ripe fruit.

340 PLSR using NIR spectra at harvest predicted DM content (Fig. 4D) and TSS content (Figure 4A) in ripe  
341 fruit better than PC (Figure 4C) and TA (Figure 4B). Our results confirm the conclusions of previous  
342 studies concerning the limited accuracy of NIR models to predict TA in mangoes that may be  
343 hampered by the number of different organic acids in this species as well as by changes in the ratio  
344 of the two main organic acids during ripening (Marques *et al.*, 2016; Nordey *et al.*, 2017; Schmilovitch  
345 *et al.*, 2000). Similar results have also been reported in apple (McGlone *et al.*, 2002a) and in passion  
346 fruit (Maniwaru *et al.*, 2014). The TA and PC of ripe fruit were found to be best predicted in PLSR  
347 using NIR measurements at 1600-1800 nm. Previous studies using NIRS showed that the  $\beta$  carotene  
348 content in mango (Rungpichayapichet *et al.*, 2015) and Chinese kale (Chen *et al.*, 2009) was related  
349 to absorbance of around 1750 nm. This is in agreement with linear regressions showing that  
350 titratable acidity in ripe fruit is linked to PC at harvest.

351 The NIR models developed in the present study succeeded in predicting fruit shelf life with an  
352 average error of less than two days. These results are satisfactory compared with the measurement  
353 error of shelf life using fruit respiration, which is around one day. The results in Figure 4J show that  
354 the region of the spectrum near 800 nm is important to predict fruit shelf life. This region is related  
355 to absorption by chlorophyll pigments, which are known to be a reliable descriptor of mango  
356 maturity (Lechaudel *et al.*, 2010). The chlorophyll content in mango peel is known to increase during  
357 the first stages of mango development and to decrease during fruit ripening (Medlicott *et al.*, 1986).

358 Although several authors used NIR measurements to predict the stage of maturity of mangoes  
359 (Cortés *et al.*, 2016; Nagle *et al.*, 2010; Rungpichayapichet *et al.*, 2016; Subedi *et al.*, 2007), to our  
360 knowledge, this is the first report on the use of NIRS to predict fruit shelf life at harvest. It should be  
361 noted that the fruit shelf life of fruit predicted in the present study is for storage at 20 °C and 80%  
362 RH. In any other post-harvest conditions, PLSR would need to be recalibrated to predict fruit shelf  
363 life. Our results provide evidence that NIR models can help predict some quality traits of ripe fruit,

364 i.e. dry matter, TSS content and shelf life. Future studies should use more samples to improve the  
365 robustness and the accuracy of the models, especially for predictions of TA of ripe fruit at harvest.

### 366 **Conclusions**

367 The quality and the maturity of fruit are two notions that are often confused since similar indicators  
368 are used to assess them. The present work used NIR models to analyze the relationship between  
369 mango quality traits at harvest and after ripening. Our results provide evidence that fruit DM content  
370 at harvest is a useful indicator of TSS content in fruit after ripening but not of TA or PC. Pulp color at  
371 harvest was found to be the best indicator of fruit shelf life because of its relative insensitivity to  
372 growing conditions. The NIR models we developed enabled prediction of fruit shelf life, TSS content  
373 and DM content in ripe fruit. Prediction accuracy was nevertheless lower for fruit acidity and PC.

374

375

376

377

378

379

380

381

382

383

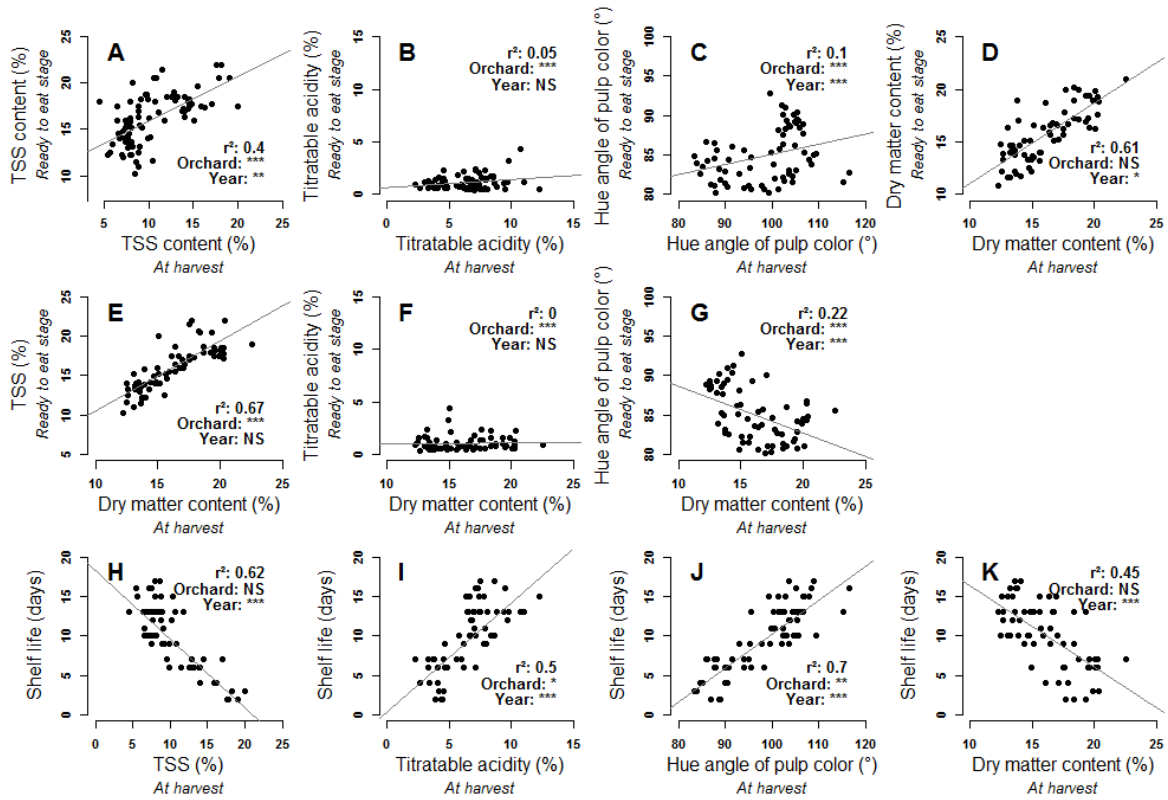
384

385

386

387

388 **Tables and figures**



389

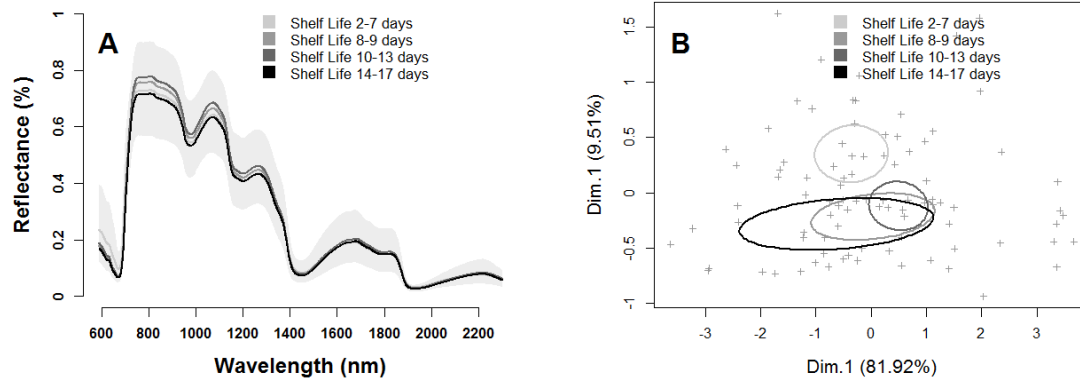
390 **Figure 1:** Relationship between (i) quality traits measured at harvest and after ripening (A to D), (ii)

391 quality traits measured after ripening and dry matter content measured at harvest (E to G) and (iii)

392 shelf life and quality traits measured at harvest (H to K). Correlation coefficients ( $r^2$ ) are indicated in

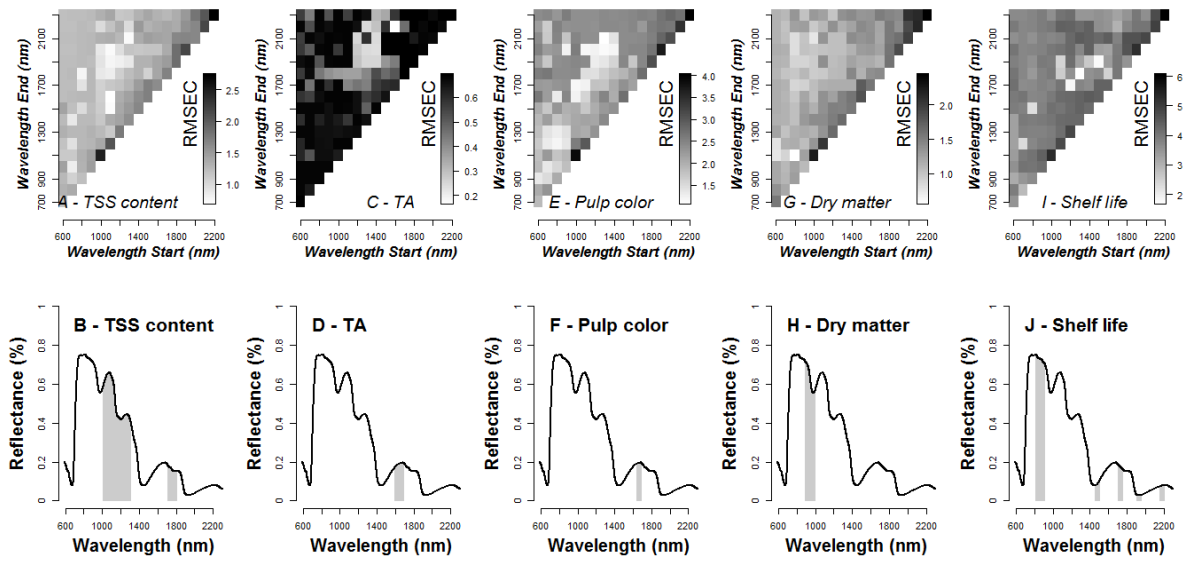
393 the figures and asterisks indicate whether years and orchard significantly impact relationships

394 displayed with p. values of 0.001 \*\*\*, 0.01\*\*, and 0.05\*.



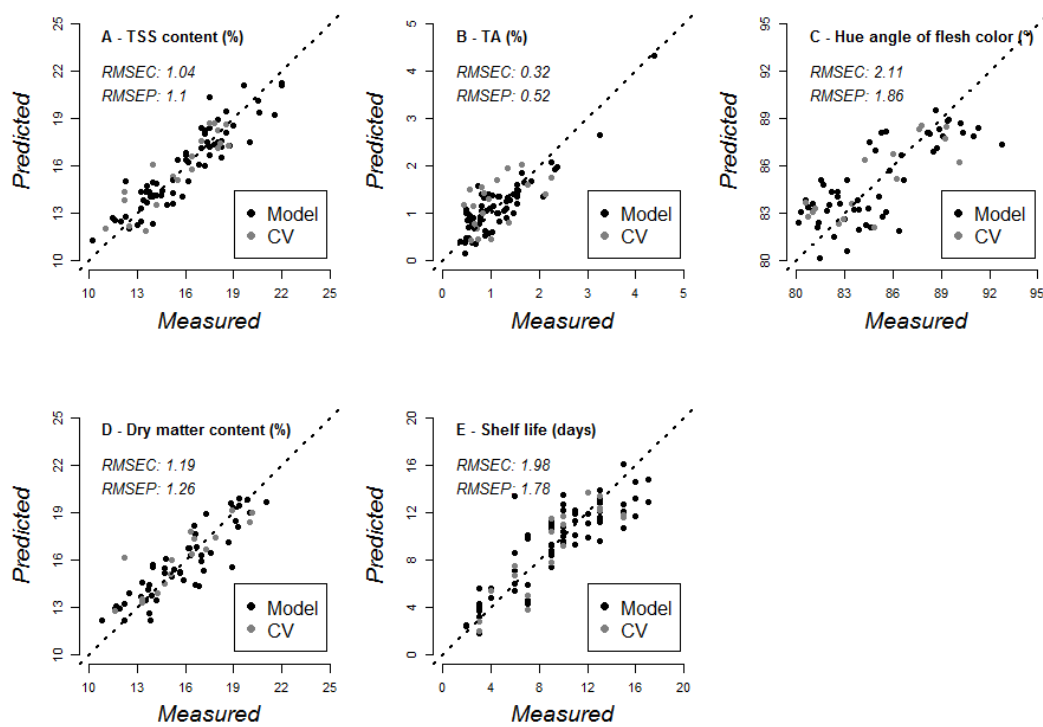
395

396 **Figure 2:** Raw NIR spectra acquired on the peel at the apex of the mango fruit at harvest with  
 397 averages calculated by range of self-life (A) and their scores in the principal component analysis (B).  
 398 Average fruit shelf life is shown as supplementary categorical variables with their confidence ellipses  
 399 at 95%.



400

401 **Figure 3:** Prediction performances of the selected PLSR regressions, in terms of root mean square  
 402 standard error of calibration (RMSEC), for different wavelength windows (from a starting point to an  
 403 end point) and the NIR regions selected for percentage total soluble solid (TSS) content (A-B),  
 404 percentage titratable acidity (TA) (C-D), percentage pulp color (PC) (E-F), percentage dry matter  
 405 (DM) content (G-H) and shelf life (in days) in the best models (I-J).



406

407 **Figure 4:** Accuracy of selected partial least square (PLS) regressions in predicting total soluble solid  
 408 (TSS) content (A), titratable acidity (TA) (B), pulp color (C), dry matter content (D) and shelf life (E)  
 409 with calibration and validation data sets.

410

411 **Table 1:** Accuracy of linear regressions based on quality attributes measured at harvest: percentage  
 412 titratable acidity (TA), percentage dry matter content (DM), percentage TSS content, and hue angle  
 413 of the pulp color (in °) to predict the shelf life and quality of fruit after ripening.

Quality traits in ripe fruit	Quality traits measured at harvest	RMSEC	RMSEP
Titratable acidity	<i>Titratable acidity</i>	0.13	0.09
	<i>Dry matter content</i>	0.13	0.1
	<i>TSS content</i>	0.13	0.1
	<i>Pulp color</i>	0.13	0.1
	<i>All</i>	0.1	0.16
	<i>Pulp color &amp; titratable acidity</i>	<b>0.12</b>	<b>0.07</b>
Pulp color	<i>Titratable acidity</i>	3.21	3.60
	<i>Dry matter content</i>	<b>2.84</b>	<b>3.17</b>
	<i>TSS content</i>	3.14	3.30
	<i>Pulp color</i>	3.13	3.23
	<i>All</i>	2.16	3.91
Dry matter content	<i>Titratable acidity</i>	2.26	1.84
	<i>Dry matter content</i>	<b>1.67</b>	<b>1.06</b>
	<i>TSS content</i>	2.03	1.78
	<i>Pulp color</i>	1.84	1.50
	<i>All</i>	1.22	1.62
TSS content	<i>Titratable acidity</i>	2.47	2.07
	<i>Dry matter content</i>	1.53	1.22
	<i>TSS content</i>	2.13	1.82
	<i>Pulp color</i>	1.91	1.49
	<i>All</i>	1.06	1.57
	<i>Titratable acidity &amp; Dry matter content &amp; Pulp color</i>	<b>1.41</b>	<b>1.18</b>
Shelf life	<i>Titratable acidity</i>	2.83	2.57
	<i>Dry matter content</i>	3.04	2.08
	<i>TSS content</i>	2.55	2.05
	<i>Pulp color</i>	<b>2.27</b>	<b>1.56</b>
	<i>All</i>	1.91	1.79

414

415

416

417 **Table 2:** Capacity of partial least squares regressions (PLSR) to predict quality of fruit after ripening and their shelf life at harvest using NIR spectra  
 418 with different variable selection and preprocessing methods. The root mean square error (RMSE) was used as an indicator to evaluate the predictive  
 419 performance of PLSR for calibration (RMSEC) and prediction (RMSEP) datasets.

		DM (%)			TSS content (%)			Titratable acidity (%)			Hue angle of pulp color (°)			Shelf life (days)		
		RMSEC	RMSEV	Factors	RMSEC	RMSEV	Factors	RMSEC	RMSEV	Factors	RMSEC	RMSEV	Factors	RMSEC	RMSEV	Factors
<i>Raw spectra</i>	<i>No variable selection</i>	0.91	1.57	9.00	1.12	1.42	11.00	0.17	0.68	20.00	2.14	2.90	5.00	2.02	1.75	12.00
	<i>IPLS_Backward_10</i>	1.45	1.77	8.00	1.93	1.68	3.00	0.66	0.50	1.00	2.74	2.76	3.00	3.43	2.62	3.00
	<i>IPLS_Backward_25</i>	1.44	1.42	4.00	2.14	2.21	3.00	0.67	0.52	1.00	2.78	3.12	3.00	3.36	2.29	2.00
	<i>IPLS_Backward_50</i>	1.40	2.05	7.00	2.19	2.13	5.00	0.67	0.51	1.00	1.72	2.75	7.00	3.26	2.61	4.00
	<i>IPLS_Backward_100</i>	<b>1.19</b>	<b>1.26</b>	<b>5.00</b>	1.54	1.44	6.00	0.46	0.46	6.00	2.21	2.57	4.00	2.78	1.94	5.00
	<i>IPLS_Stepwise_10</i>	1.41	1.46	7.00	1.11	1.69	10.00	0.52	0.66	7.00	1.99	3.93	7.00	2.50	1.48	7.00
	<i>IPLS_Stepwise_25</i>	1.25	1.83	6.00	1.09	2.01	11.00	0.22	0.54	15.00	1.86	2.78	7.00	2.82	2.14	4.00
	<i>IPLS_Stepwise_50</i>	1.38	1.98	5.00	0.99	1.27	11.00	0.63	0.45	3.00	<b>2.11</b>	<b>1.86</b>	<b>4.00</b>	2.46	1.84	7.00
	<i>IPLS_Stepwise_100</i>	0.63	1.69	13.00	1.64	1.59	6.00	<b>0.32</b>	<b>0.52</b>	<b>12.00</b>	1.87	2.54	6.00	2.48	1.76	4.00
<i>First derivative</i>	<i>No variable selection</i>	0.88	1.62	7.00	1.24	1.66	6.00	0.21	0.58	15.00	1.53	2.38	9.00	0.94	2.62	18.00
	<i>IPLS_Backward_10</i>	1.13	1.53	6.00	1.37	1.59	9.00	0.61	0.53	3.00	2.67	3.09	4.00	2.69	2.66	4.00
	<i>IPLS_Backward_25</i>	2.38	2.16	2.00	2.12	2.40	3.00	0.66	0.53	1.00	1.63	2.06	12.00	3.55	3.15	3.00
	<i>IPLS_Backward_50</i>	1.44	1.96	10.00	2.13	2.21	4.00	0.63	0.48	2.00	2.52	2.49	6.00	2.96	3.53	6.00
	<i>IPLS_Backward_100</i>	1.47	1.31	3.00	1.84	1.27	3.00	0.62	0.45	5.00	2.29	2.39	7.00	2.21	2.19	9.00
	<i>IPLS_Stepwise_10</i>	0.71	1.87	10.00	1.25	1.78	9.00	0.54	0.48	6.00	2.34	2.57	8.00	2.19	2.12	10.00
	<i>IPLS_Stepwise_25</i>	1.14	1.93	10.00	0.99	1.48	11.00	0.62	0.45	3.00	2.24	3.68	5.00	2.66	2.58	7.00
	<i>IPLS_Stepwise_50</i>	1.05	1.68	9.00	1.13	1.15	9.00	0.51	0.54	5.00	2.16	2.72	4.00	<b>1.98</b>	<b>1.78</b>	<b>5.00</b>
	<i>IPLS_Stepwise_100</i>	1.14	1.27	5.00	<b>1.04</b>	<b>1.10</b>	<b>9.00</b>	0.35	0.53	10.00	1.92	2.28	7.00	2.03	1.64	6.00
<i>Second derivative</i>	<i>No variable selection</i>	0.86	1.62	8.00	1.01	1.20	9.00	0.21	0.55	14.00	0.29	3.07	20.00	0.66	2.65	19.00
	<i>IPLS_Backward_10</i>	1.49	2.12	4.00	1.62	1.80	6.00	0.61	0.46	4.00	2.26	3.29	5.00	2.50	1.62	3.00
	<i>IPLS_Backward_25</i>	1.38	1.81	7.00	2.54	2.27	2.00	0.62	0.49	2.00	2.20	2.84	5.00	2.47	1.79	3.00
	<i>IPLS_Backward_50</i>	1.39	1.65	5.00	1.35	1.26	6.00	0.66	0.47	2.00	2.76	2.86	1.00	2.72	2.45	5.00
	<i>IPLS_Backward_100</i>	1.55	1.87	5.00	1.86	1.45	3.00	0.62	0.47	3.00	1.95	2.11	7.00	2.92	2.19	3.00
	<i>IPLS_Stepwise_10</i>	1.21	1.66	7.00	1.25	1.82	11.00	0.57	0.60	6.00	1.93	2.94	9.00	1.81	2.65	12.00
	<i>IPLS_Stepwise_25</i>	1.39	1.60	3.00	1.00	1.75	13.00	0.63	0.47	1.00	1.56	3.45	10.00	2.40	2.17	6.00
	<i>IPLS_Stepwise_50</i>	1.13	1.67	5.00	1.12	1.14	7.00	0.61	0.50	2.00	1.84	3.05	9.00	2.36	1.41	4.00
	<i>IPLS_Stepwise_100</i>	1.31	1.36	5.00	1.17	1.11	5.00	0.65	0.53	1.00	1.85	2.44	4.00	2.12	1.86	7.00

421 **References**

- 422 Andersen, C.M., Bro, R., 2010. Variable selection in regression—a tutorial. *Journal of Chemometrics*  
423 24, 728-737.
- 424 Chen, X., Wu, J., Zhou, S., Yang, Y., Ni, X., Yang, J., Zhu, Z., Shi, C., 2009. Application of near-infrared  
425 reflectance spectroscopy to evaluate the lutein and  $\beta$ -carotene in Chinese kale. *Journal of food*  
426 *composition and analysis* 22, 148-153.
- 427 Cornillon, P.A., 2010. *Statistiques avec R: 2e édition augmentée*. Presses universitaires de Rennes.
- 428 Cortés, V., Ortiz, C., Aleixos, N., Blasco, J., Cubero, S., Talens, P., 2016. A new internal quality index for  
429 mango and its prediction by external visible and near-infrared reflection spectroscopy. *Postharvest*  
430 *Biology and Technology* 118, 148-158.
- 431 Etienne, A., Génard, M., Bancel, D., Benoit, S., Bugaud, C., 2013. A model approach revealed the  
432 relationship between banana pulp acidity and composition during growth and post harvest ripening.  
433 *Scientia Horticulturae* 162, 125-134.
- 434 Génard, M., Gouble, B., 2005. ETHY. A Theory of Fruit Climacteric Ethylene Emission. *Plant Physiology*  
435 139, 531-545.
- 436 Jha, S.N., Jaiswal, P., Narsaiah, K., Gupta, M., Bhardwaj, R., Singh, A.K., 2012a. Non-destructive  
437 prediction of sweetness of intact mango using near infrared spectroscopy. *Scientia Horticulturae* 138,  
438 171-175.
- 439 Jha, S.N., Jaiswal, P., Narsaiah, K., Gupta, M., Bhardwaj, R., Singh, A.K., 2012b. Non-destructive  
440 prediction of sweetness of intact mango using near infrared spectroscopy. *Scientia Horticulturae* 138,  
441 171-175.
- 442 Jha, S.N., Kingsly, A.R.P., Chopra, S., 2006. Non-destructive determination of firmness and yellowness  
443 of mango during growth and storage using visual spectroscopy. *Biosystems Engineering* 94, 397-402.
- 444 Jha, S.N., Narsaiah, K., Jaiswal, P., Bhardwaj, R., Gupta, M., Kumar, R., Sharma, R., 2014.  
445 Nondestructive prediction of maturity of mango using near infrared spectroscopy. *Journal of Food*  
446 *Engineering* 124, 152-157.
- 447 Joas, J., Caro, Y., Lechaudel, M., 2009. Comparison of postharvest changes in mango (cv Cogshall)  
448 using a Ripening class index (Rci) for different carbon supplies and harvest dates. *Postharvest biology*  
449 *and technology* 54, 25-31.
- 450 Joas, J., Vulcain, E., Desvignes, C., Morales, E., Léchaudel, M., 2012. Physiological age at harvest  
451 regulates the variability in postharvest ripening, sensory and nutritional characteristics of mango  
452 (*Mangifera indica* L.) cv. Cogshall due to growing conditions. *Journal of the Science of Food and*  
453 *Agriculture* 92, 1282-1290.
- 454 Joas, J., Vulcain, E., Léchaudel, M., 2010. Effect of fruit position in the canopy on physiological age  
455 and physicochemical composition of mango 'Cogshall', IX International Mango Symposium 992, pp.  
456 123-128.
- 457 Jordan, R.B., Walton, E.F., Klages, K.U., Seelye, R.J., 2000. Postharvest fruit density as an indicator of  
458 dry matter and ripened soluble solids of kiwifruit. *Postharvest Biology and Technology* 20, 163-173.
- 459 Kapse, B.M., Katrodia, J., 1996. Ripening behaviour of 'Kesar' mangoes in relation to specific gravity, V  
460 International Mango Symposium 455, pp. 669-678.
- 461 Lê, S., Josse, J., Husson, F., 2008. FactoMineR: an R package for multivariate analysis. *Journal of*  
462 *statistical software* 25, 1-18.
- 463 Lebrun, M., Plotto, A., Goodner, K., Ducamp, M.-N., Baldwin, E., 2008. Discrimination of mango fruit  
464 maturity by volatiles using the electronic nose and gas chromatography. *Postharvest Biology and*  
465 *Technology* 48, 122-131.
- 466 Léchaudel, M., Joas, J., 2007. An overview of preharvest factors influencing mango fruit growth,  
467 quality and postharvest behaviour. *Brazilian Journal of Plant Physiology* 19, 287-298.
- 468 Léchaudel, M., Joas, J., Caro, Y., Génard, M., Jannoyer, M., 2005. Leaf:fruit ratio and irrigation supply  
469 affect seasonal changes in minerals, organic acids and sugars of mango fruit. *Journal of the Science of*  
470 *Food and Agriculture* 85, 251-260.

471 Lechaudel, M., Urban, L., Joas, J., 2010. Chlorophyll Fluorescence, a Nondestructive Method To  
472 Assess Maturity of Mango Fruits (Cv. 'Cogshall') without Growth Conditions Bias. *Journal of*  
473 *Agricultural and Food Chemistry* 58, 7532-7538.

474 Léchaudel, M., Vercambre, G., Lescourret, F., Normand, F., Génard, M., 2007. An analysis of elastic  
475 and plastic fruit growth of mango in response to various assimilate supplies. *Tree Physiology* 27, 219-  
476 230.

477 Lescourret, F., Moitrier, N., Valsesia, P., Génard, M., 2011. QualiTree, a virtual fruit tree to study the  
478 management of fruit quality. I. Model development. *Trees* 25, 519-530.

479 Litz, R.E., 2009. *The Mango*, 2nd Edition: Botany, Production and Uses. Wiley Online Library.

480 Liu, H.-F., Génard, M., Guichard, S., Bertin, N., 2007. Model-assisted analysis of tomato fruit growth  
481 in relation to carbon and water fluxes. *Journal of Experimental Botany* 58, 3567-3580.

482 Lobit, P., Génard, M., Wu, B.H., Soing, P., Habib, R., 2003. Modelling citrate metabolism in fruits:  
483 responses to growth and temperature. *Journal of Experimental Botany* 54, 2489-2501.

484 Lumley, T., Miller, A., 2009. Leaps: regression subset selection. R package version 2.9. Online at  
485 <http://CRAN.R-project.org/package=leaps>.

486 Maniwaru, P., Nakano, K., Boonyakiat, D., Ohashi, S., Hiroi, M., Tohyama, T., 2014. The use of visible  
487 and near infrared spectroscopy for evaluating passion fruit postharvest quality. *Journal of Food*  
488 *Engineering* 143, 33-43.

489 Marques, E.J.N., de Freitas, S.T., Pimentel, M.F., Pasquini, C., 2016. Rapid and non-destructive  
490 determination of quality parameters in the 'Tommy Atkins' mango using a novel handheld near  
491 infrared spectrometer. *Food Chemistry* 197, 1207-1214.

492 McAtee, P., Karim, S., Schaffer, R., David, K., 2013. A dynamic interplay between phytohormones is  
493 required for fruit development, maturation, and ripening. *Frontiers in plant science* 4, 79.

494 McGlone, V.A., Jordan, R.B., Martinsen, P.J., 2002a. Vis/NIR estimation at harvest of pre-and post-  
495 storage quality indices for 'Royal Gala' apple. *Postharvest Biology and Technology* 25, 135-144.

496 McGlone, V.A., Jordan, R.B., Seelye, R., Martinsen, P.J., 2002b. Comparing density and NIR methods  
497 for measurement of Kiwifruit dry matter and soluble solids content. *Postharvest Biology and*  
498 *Technology* 26, 191-198.

499 Medicott, A.P., Bhogal, M., Reynolds, S.B., 1986. Changes in peel pigmentation during ripening of  
500 mango fruit (*Mangifera indica* var. Tommy Atkins). *Annals of Applied Biology* 109, 651-656.

501 Medicott, A.P., Thompson, A.K., 1985. Analysis of sugars and organic acids in ripening mango fruits  
502 (*Mangifera indica* L. var Keitt) by high performance liquid chromatography. *Journal of the Science of*  
503 *Food and Agriculture* 36, 561-566.

504 Mevik, B.-H., Wehrens, R., 2007. The pls package: principal component and partial least squares  
505 regression in R. *Journal of Statistical Software* 18, 1-24.

506 Nagle, M., Mahayothee, B., Rungpichayapichet, P., Janjai, S., Müller, J., 2010. Effect of irrigation on  
507 near-infrared (NIR) based prediction of mango maturity. *Scientia Horticulturae* 125, 771-774.

508 Nicolaï, B.M., Beullens, K., Bobelyn, E., Peirs, A., Saeys, W., Theron, K.I., Lammertyn, J., 2007.  
509 Nondestructive measurement of fruit and vegetable quality by means of NIR spectroscopy: A review.  
510 *Postharvest Biology and Technology* 46, 99-118.

511 Nordey, T., Joas, J., Davrieux, F., Chillet, M., Léchaudel, M., 2017. Robust NIRS models for non-  
512 destructive prediction of mango internal quality. *Scientia Horticulturae* 216, 51-57.

513 Nordey, T., Léchaudel, M., Génard, M., Joas, J., 2014. Spatial and temporal variations in mango  
514 colour, acidity, and sweetness in relation to temperature and ethylene gradients within the fruit.  
515 *Journal of plant physiology* 171, 1555-1563.

516 Nordey, T., Léchaudel, M., Génard, M., Joas, J., 2016. Factors affecting ethylene and carbon dioxide  
517 concentrations during ripening: Incidence on final dry matter, total soluble solids content and acidity  
518 of mango fruit. *Journal of Plant Physiology* 196, 70-78.

519 Palmer, J.W., Harker, F.R., Tustin, D.S., Johnston, J., 2010. Fruit dry matter concentration: a new  
520 quality metric for apples. *Journal of the Science of Food and Agriculture* 90, 2586-2594.

521 Poiroux-Gonord, F., Fanciullino, A.L., Bert, L., Urban, L., 2012. Effect of fruit load on maturity and  
522 carotenoid content of clementine (*Citrus clementina* Hort. ex Tan.) fruits. *Journal of the Science of*  
523 *Food and Agriculture* 92, 2076-2083.

524 R Development Core Team, 2012. R: A Language and Environment for Statistical Computing.  
525 Rosalie, R., Joas, J., Deytieux-Belleau, C., Vulcain, E., Payet, B., Dufossé, L., Léchaudel, M., 2015.  
526 Antioxidant and enzymatic responses to oxidative stress induced by pre-harvest water supply  
527 reduction and ripening on mango (*Mangifera indica* L. cv. 'Cogshall') in relation to carotenoid  
528 content. *Journal of Plant Physiology* 184, 68-78.

529 Rungpichayapichet, P., Mahayothee, B., Khuwijitjaru, P., Nagle, M., Muller, J., 2015. Non-destructive  
530 determination of beta-carotene content in mango by near-infrared spectroscopy compared with  
531 colorimetric measurements. *Journal of Food Composition and Analysis* 38, 32-41.

532 Rungpichayapichet, P., Mahayothee, B., Nagle, M., Khuwijitjaru, P., Müller, J., 2016. Robust NIRS  
533 models for non-destructive prediction of postharvest fruit ripeness and quality in mango. *Postharvest*  
534 *Biology and Technology* 111, 31-40.

535 Saranwong, S., Sornsrivichai, J., Kawano, S., 2004. Prediction of ripe-stage eating quality of mango  
536 fruit from its harvest quality measured nondestructively by near infrared spectroscopy. *Postharvest*  
537 *Biology and Technology* 31, 137-145.

538 Schmilovitch, Z.e., Mizrach, A., Hoffman, A., Egozi, H., Fuchs, Y., 2000. Determination of mango  
539 physiological indices by near-infrared spectrometry. *Postharvest Biology and Technology* 19, 245-  
540 252.

541 Song, J., Deng, W., Beaudry, R.M., Armstrong, P.R., 1997. Changes in Chlorophyll Fluorescence of  
542 Apple Fruit during Maturation, Ripening, and Senescence. *HortScience* 32, 891-896.

543 Stevens, A., Ramirez-Lopez, L., 2013. Miscellaneous functions for processing and sample selection of  
544 vis-NIR diffuse reflectance data.

545 Subedi, P., Walsh, K.B., Owens, G., 2007. Prediction of mango eating quality at harvest using short-  
546 wave near infrared spectrometry. *Postharvest Biology and Technology* 43, 326-334.

547 Urbano Bron, I., Vasconcelos Ribeiro, R., Azzolini, M., Pedro Jacomino, A., Caruso Machado, E., 2004.  
548 Chlorophyll fluorescence as a tool to evaluate the ripening of 'Golden' papaya fruit. *Postharvest*  
549 *Biology and Technology* 33, 163-173.

550 Vasquez-Caicedo, A.L., Sruamsiri, P., Carle, R., Neidhart, S., 2005. Accumulation of All-trans- $\beta$ -  
551 carotene and Its 9-cis and 13-cis Stereoisomers during Postharvest Ripening of Nine Thai Mango  
552 Cultivars. *Journal of Agricultural and Food Chemistry* 53, 4827-4835.

553